



**HAL**  
open science

## Efficient 3D Reconstruction of H&E Whole Slide Images in Melanoma

Janan Arslan, Mehdi Ounissi, Haocheng Luo, Matthieu Lacroix, Pierrick Dupré, Pawan Kumar, Arran Hodgkinson, Sarah Dandou, Romain M Larive, Christine Pignodel, et al.

► **To cite this version:**

Janan Arslan, Mehdi Ounissi, Haocheng Luo, Matthieu Lacroix, Pierrick Dupré, et al.. Efficient 3D Reconstruction of H&E Whole Slide Images in Melanoma. SPIE Medical Imaging 2023, Feb 2023, San Diego, California, United States. hal-03834014v1

**HAL Id: hal-03834014**

**<https://hal.science/hal-03834014v1>**

Submitted on 28 Oct 2022 (v1), last revised 9 Mar 2023 (v2)

**HAL** is a multi-disciplinary open access archive for the deposit and dissemination of scientific research documents, whether they are published or not. The documents may come from teaching and research institutions in France or abroad, or from public or private research centers.

L'archive ouverte pluridisciplinaire **HAL**, est destinée au dépôt et à la diffusion de documents scientifiques de niveau recherche, publiés ou non, émanant des établissements d'enseignement et de recherche français ou étrangers, des laboratoires publics ou privés.

# 3D Reconstruction of H&E Whole Slide Images in Melanoma

J. Arslan, H. Luo, M. Lacroix, P. Dupré, P. Kumar, A. Hodgkinson, S. Dandou, R. Larive, C. Pignodel, L. Le Cam, O. Radulescu, D. Racoceanu

Sorbonne Université, Institut du Cerveau - Paris Brain Institute - ICM, CNRS, Inria, Inserm, AP-HP, Hôpital de la Pitié Salpêtrière, Paris, France

Laboratory of Pathogen Host Interactions, Université de Montpellier, CNRS, Montpellier, France

Quantitative Biology & Medicine, Living Systems Institute, University of Exeter, Exeter, United Kingdom

Institut de Recherche en Cancérologie de Montpellier (IRCM), INSERM, Université de Montpellier, Institut régional du Cancer de Montpellier, Montpellier, France

**Keywords:** cutaneous melanoma, whole slide images, hematoxylin and eosin, 3D reconstruction, vascular reconstruction, personalized medicine

## 1. PURPOSE OF THE STUDY

Cutaneous melanoma has rapidly evolved to become one of the most fatal forms of cancers today, accounting for approximately 57,000 deaths worldwide as of 2020 (Arnold *et al.*, JAMA Dermatol 2022). Management of late-stage, metastatic melanoma is challenging. Despite rigorous therapies, clinical prognosis remains poor with an average survival time of 8 months (Garbe *et al.*, Oncologist 2011)

The infiltration of resident host cells by the cancer can stimulate molecular, cellular, and physical changes within the host tissue, creating a tumor microenvironment that is conducive to the survival and proliferation of melanoma. Furthermore, cancer cells have the ability to rewire themselves under changing environmental conditions (e.g., poorly vascularized and hypoxic tumor microenvironment), and thus adapt and thrive within altered metabolic states.

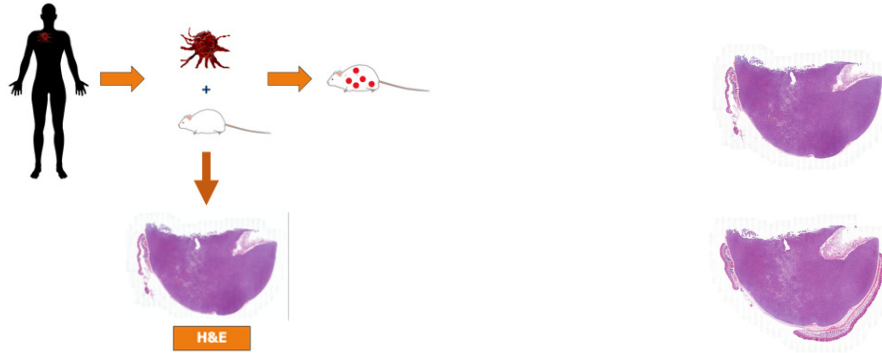
In this study, our primary assumption is that chemotherapeutic resistance stems from a series of non-genetic transitions and changed metabolic states. We propose a 3D vascular pipeline based on artificial intelligence (AI) algorithms to capture and assess evolving metabolic states. The 3D reconstruction of blood vessels can be used to explicate how characteristics such as vascular shape, size and bifurcations differ in alternate metabolic states, and thus can be used in predicting treatment efficacy. The proposed pipeline has a multi-function purpose: in addition to understanding the characteristics of the vascular network through reconstruction, we also automate previously human-run and manual pathology grading systems that are time consuming and arduous.

The pipeline was designed for Whole Slide Images (WSIs) of melanoma tumors from Patient-Derived Xenograft (PDX) mouse models, specifically Hematoxylin and Eosin (H&E)-stained pathology slides. In this study, we elucidate the steps of our pipeline, provide qualitative and quantitative assessment, and discuss WSI-related challenges (notorious and plenty owing to the size and depth of information in WSIs), and the solutions we have utilized to improve the efficiency and adaptability of our 3D reconstruction.

---

Further author information: (Send correspondence to Janan Arslan)

J.A.: E-mail: janan.arslan@icm-institute.org, Telephone: +33 (0)6 75 22 39 53



(a) Complete PDX model illustration.

(b) Sample H&E slide with two tissue sections.

Figure 1: Human tumors are engrafted onto immunodeficient mice and grown. Mice-harvested samples then undergo serial sectioning. Slides stained with hematoxylin and eosin (H&E) are digitized into whole slide images (WSIs).

## 2. METHOD

### 2.1 Data preparation

#### a. Raw data

The PDX model is illustrated in Fig. 1a. Cutaneous melanoma tumors were extracted from humans during biopsy, then implanted in mice for growth, extraction and evaluation. PDX samples underwent serial sectioning at every  $12\mu\text{m}$  over a depth of  $2\text{mm}$  and were stained with H&E. Each tissue had a thickness of  $4\mu\text{m}$ . This sectioning protocol resulted in gaps between each tissue section, which were imputed using interpolation methods (refer to Section 2.2(d)). Slides were digitized into MIRAX format. Each slide contained two tissue sections (i.e., top and bottom) as shown in Fig. 1b; this method was used to expedite data acquisition time and reduce production costs. A total of 120 slides (240 tissues sections) were available. Blood vessels were annotated by an expert pathologist (co-author *CP*) using the open-source software QuPath.

#### b. Sampling

In preparation for training using deep learning methods, WSIs along with their annotated counterparts were exported as tiles/patches from QuPath. Patches were sized  $512 \times 512$  (with size selection based on preliminary experimentation with various patch sizes) and were exported at their highest resolution ( $0.25\ \mu\text{m}$  per pixel). A total of 1000 patches with positive (i.e., presence of blood vessels) and negative (i.e., background/other molecular markers) cases were captured.

### 2.2 3D Reconstruction Pipeline

#### a. 2D Blood Vessel Segmentation

A segmentation algorithm was trained using the U-Net architecture. Data were trained and tested using a 5-fold cross-validation approach, with each fold split into 80% training and 20% test. The hyperparameters included: batch size=32, the ADAM optimizer, learning rate= $3 \times 10^{-5}$ , epoch=1000, and the binary cross entropy Dice loss function (BCE DICE). The BCE DICE was chosen based on its ability to better discern vascular boundaries as compared to other loss functions.

#### b. 2D Segmentation Evaluation

The evaluation metrics used were BCE DICE, the mean absolute error (MAE), accuracy (ACC), Dice coefficient (DICE), Dice Loss (i.e.,  $1 - \text{DICE}$ ; DICE LOSS), the  $F_1$ -score, Precision (PREC), recall (REC), specificity (SPEC) and Matthews Correlation Coefficient (MCOR).

#### c. Image Registration

Due to the considerable variability in WSIs (i.e., tissue shift, background noise, etc.), images were centered, cropped, and noisy backgrounds were removed prior to registration. Furthermore, the epidermis was inpainted

using a secondary trained U-Net model, as the epidermis hindered the performance of the registration and its presence provided little value for the final vascular reconstruction. These pre-processing steps created a better uniformity between images and improved registration output. The symmetric, intensity-based affine registration framework proposed by Öfverstedt *et al.* (IEEE 2019) was utilized for the registration. Images were registered in pairs and in a sequential order. Performance across all registered pairs was assessed with the Structural Similarity Index (SSIM).

d. *3D Rendering and Interpolation*

For a complete 3D reconstruction, a hybrid solution was created using rendering and interpolation, where rendering stacks existing data to create a preliminary vascular volume while the interpolation imputes the gaps between the H&E rendered tissues sections. Rendering was achieved with marching cubes. The shape- and distance-based method proposed by Schenk *et al.* (MICCAI 2000) was used for interpolation.

e. *Overall Pipeline*

Fig. 2 provides an overall outline of the 3D reconstruction pipeline. Images are (A) exported, (B) split into top and bottom tissues, (C) crop centred, inpainted, and cleaned via the removal of the noisy background, (D) registered in a pairwise fashion sequentially, (E & F) and undergo patch-level segmentation to produce complete, segmented WSIs (G). All segmented WSIs undergo rendering and interpolation to produce a final 3D vascular model (H & I).

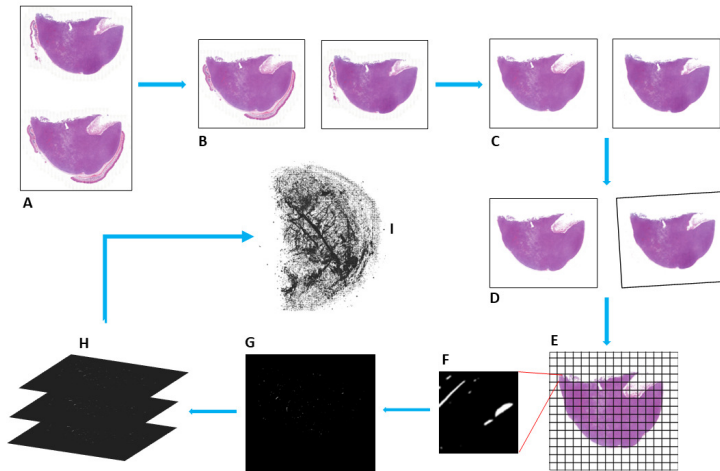


Figure 2: Overall pipeline for 3D vascular reconstruction from H&E-stained WSIs.

### 3. RESULTS

2D segmentation performs generally well as demonstrated in Table 1, with DICE > 80% in training and test results. The 3D reconstruction model illustrated in part (I) of Fig. 2 further validates this as we can qualitatively see the majority of the blood vessels (particularly the larger blood vessels, which are suggested to play an important role in understanding chemotherapeutic response). Registration performance was qualitatively and quantitatively assessed as shown in Table 2 and Fig. 3. We noticed that larger tissue sections have lower SSIMs as compared to smaller sections, despite the alignment being near-perfect visually (Fig. 3). We assume the lower SSIM is a reflection of the greater heterogeneity of blood vessels in the larger sections (i.e., many small blood vessels that do not appear across all large tissue sections). Smaller tissues, however, have larger blood vessels which appear iteratively, and thus demonstrate higher performance given the similarity in features (SSIM > 80%). The qualitative and quantitative results from this study demonstrate an overall good performance.

### 4. NEW OR BREAKTHROUGH WORK TO BE PRESENTED

We present an end-to-end approach for reconstructing a vascular 3D model based on WSIs. An original feature of our pipeline is its ability to handle sparse data, given that not all tissue sections were made readily available.

Metrics	Training		Testing	
	Mean	SD	Mean	SD
BCE DICE	0.081	0.019	0.183	0.083
MAE	0.009	0.001	0.027	0.017
ACC	0.992	0.001	0.973	0.016
DICE	0.886	0.037	0.813	0.086
DICE LOSS	0.114	0.037	0.188	0.085
REC	0.836	0.052	0.767	0.129
PREC	0.842	0.049	0.847	0.082
$F_1$	0.832	0.054	0.795	0.112
SPEC	0.996	0.001	0.985	0.015
MCOR	0.830	0.053	0.784	0.105

SD = Standard Deviation

Table 1: Average training and test results for 2D-level blood vessel segmentation based on U-Net architecture across 5-fold cross-validation.

Mean	SE	Median	SD	Min.	Max.
0.716	0.005	0.687	0.078	0.620	0.886

SE = Standard Error

SD = Standard Deviation

Table 2: Quantitative evaluation of registered images using the Structural Similarity Index (SSIM). A total of 239 SSIM results were obtained ( $n-1$ , with the first image acting as the baseline fixed image).



(a) Overlap between large tissue sections following registration. (b) Overlap between small tissue sections following registration.

Figure 3: Qualitative assessment of registered images. While visually near-perfect, variability in SSIM between larger and smaller tissues are attributable to greater heterogeneity of blood vessels in larger tissues.

This is achieved through rendering and interpolation. Furthermore, the pipeline has been built to accommodate the multitude of challenges faced with processing WSIs. These include: conducting patch-level training and segmentation; creating uniformity in the available data; and improving registration by using inpainting, crop centering, and artefact removal techniques to minimize registration-related errors. Other breakthrough components of our project include the utilization of epistemic uncertainty. This involves understanding human-related or reducible errors, and using statistical techniques to detect and minimize the impact of uncertainty on the pipeline. Our work further includes optimization via parallel processing to improve the efficiency and speed of our reconstruction process. We present the challenges and the successes of the project for posterity.

## 5. CONCLUSION

In this study, we have proven that AI can be used to develop automated and clinically operational pipelines for WSIs. Using a combination of deep learning, image processing, registration, statistical and parallel processing techniques, we can develop 3D models that are adaptable to WSI challenges and produce results which elucidate vascular networks that could predict chemotherapy efficacy in melanoma patients. This body of work can be readily extended to other biomarkers and cancer types and is not limited in its scope or application.